Supporting Information

Rational Design of Carbon/Potassium Poly(heptazine imide) Heterojunction for Enhanced Photocatalytic H_2 and H_2O_2 Evolution

Christian Mark Pelicano,[a] Jiaxin Li,[a] María Cabrero-Antonino,[b] Ingrid F. Silva, [a] Lu Peng, [a] Nadezda V. Tarakina, [a] Sergio Navalón,[b] Hermenegildo García, [b] and Markus Antonietti*[a]*

*Corresponding authors

[a]Department of Colloid Chemistry, Max Planck Institute of Colloids and Interfaces, Potsdam 14476, Germany

E-mail: christianmark.pelicano@mpikg.mpg.de, markus.antonietti@mpikg.mpg.de

[b]Departamento de Química and Instituto de Tecnología Química (CSIC-UPV), Universitat Politècnica de València, València 46022, Spain

Experimental Section

1. Chemicals

All chemicals and solvents used were purchased from different chemical suppliers (Merck, Sigma-Aldrich,) in high purity grade and were used as received. 5-aminotetrazole monohydrate was dried in a vacuum oven before using.

2. Catalyst Preparation

Synthesis of Ad-carbon:

Typically, 1 g of adenine and 10 g of CsAc were placed in a nickel crucible with a lid and heated at 800 ^oC for 2 h (heating ramp: 1 ^oC min^{-1}) under N_2 in a muffle furnace.[1] After cooling down, the carbonized products were ground and transferred to 1 M HCl aqueous solution, stirred overnight, and filtered by a Büchner funnel. The above procedures were repeated two times. The collected powders were then rinsed with deionised H_2O and dried at 60 ^oC for 4 h to get the final carbon.

Synthesis of carbon dots (CD):

3 g of citric acid and 1 g of urea were mixed in a 8 mL of deionised H_2O in a beaker and vigorously stirred until a transparent solution was obtained. Then the solution was placed inside a microwave oven and irradiated at 600 W for 10 min. The resulting solid product was then dried in an oven at 80 °C for 10 h to remove residual small molecules. The crude CD suspension was purified in a centrifuge at 8000 rpm for 1 h to remove large particles or agglomerates. The final brown aqueous solution was washed with a mixture of methanol and dichloromethane in ratios of 1:2 and 2:1. As a last step, the solution was dried to obtain the CD as a solid.[2]

Synthesis of 4-hydroxy-1H-pyrrolo[3,4-c]pyridine-1,3,6(2H,5H)-trione (HPPT):

2 g of citric acid and 3 g of urea were added to a large beaker and stirred at 120°C in an oil bath until everything is molten. The reaction mixture was reacted further at 120°C. It turned brown and increasingly solid. When it became completely solid, the product was ground and stirred for 24 h at 120°C in an oil bath.

Synthesis of KPHI and carbon material/KPHI (CM/KPHI) hybrids:

Potassium poly(heptazine imide) (KPHI) was synthesized according to a previously reported study.[3] 2.5 g of 5-aminotetrazole and 12.5 g of KCl/LiCl eutectic (0.55/0.45 ratio) were placed in a steel ball mill vessel. The mixture was then ground at operational frequency of 25 Hz for 5 min. The resulting white powder was transferred into a porcelain crucible covered with a lid, and placed in a furnace. The temperature inside the furnace was increased to 600 °C within 4 h under a flow of N_2 gas (4 L min^{-1}) and maintained this temperature for another 4 h. Subsequently, the furnace was allowed to naturally cool down to room temperature. The melt from the crucible was then transferred into a beaker with 300 mL deionized H_2O and was stirred at room temperature overnight. Then the product was vacuum-filtered and washed extensively with H_2O by centrifugation (5 x 2mL, 13 500 min^{-1}, 3 min), and dried in a vacuum oven at 60 °C for 3 h. The preparation for CM/KPHI hybrids follows the same protocol except that the carbon materials were added along with 5-aminotetrazole and the eutectic salt template.

3. Materials Characterizations

X-ray diffraction was conducted with a Rigaku SmartLab (Japan, Cu K, 0.154 nm). UV–vis absorption spectra were acquired using Shimadzu UV 2600 in diffuse reflectance mode. FTIR spectroscopy was performed using a Thermo Scientific Nicolet iD5 spectrometer with the attenuated total reflection sampling technique. Steady-state photoluminescence (PL) spectra were measured using a Jasco FP-8300 fluorescence spectrometer at an excitation wavelength of 365 nm. Time-resolved PL (TRPL) spectra were recorded on fluorescence lifetime spectrometer (FluoTime 250, PicoQuant) equipped with PDL 800-D picosecond pulsed diode laser drive. Elemental combustion analysis was performed with a vario MICRO cube CHNOS elemental analyzer (Elementar Analysensysteme GmbH). Inductively coupled plasma mass spectrometry (ICP-MS) was performed with a PerkinElmer ICP-OES Optima 8000. Transmission electron microscopy (TEM) images were taken using JEOL JEM F200 and a double Cs corrected JEOL JEM-ARM200F operated at 80kV and equipped with a cold-field emission gun and high-angle silicon drift Energy Dispersive X-ray (EDX) detector (Jeol JED-2300 100 mm^2, Japan) (solid angle up to 0.98 steradians with a detection area of 100 mm^2). Annular Dark Field Scanning Transmission Electron Microscopy (ADF – STEM) images were collected at a probe convergence semi-angle of 25 mrad. The morphologies of the samples were observed using a scanning electron microscope (SEM) (Zeiss LEO 1550-Gemini) equipped with an EDX (Oxford Instruments X-MAX). Nitrogen adsorption and desorption isotherms were measured at 77 K using a Quantachrome Quadrasorb SI apparatus. The samples were degassed at 150 °C under vacuum (0.5 Torr) for 20 h prior to each measurement. The specific surface area of each material was calculated from the adsorption branch data ($P/P_0 < 0.3$) using the Brunauer−Emmett−Teller (BET) method.

4. Photocatalytic Experiments

Photocatalytic H_2 Evolution

Sacrificial photocatalytic H_2 evolution experiments were performed in a closed system equipped with a pressure detector to monitor the pressure build-up of the gases evolving during photocatalytic reactions. White LED (50 W, $\lambda > 420$ nm), purple LED (50 W, $\lambda = 410$ nm) and a green LED (50 W, $\lambda = 535$ nm) were used as light source for the photocatalytic evaluation. A total volume of 38 mL was used and the temperature during the reaction was maintained at

295 K by a water circulator unit. Typically, 50 mg of photocatalyst powder was dispersed in a 38 mL mixture of DI H_2O and TEOA with a volume ratio of 9:1, which was degassed beforehand to remove the dissolved O_2 in the solution. The reactor was then illuminated from the side for 6 h. 3 wt% of Pt cocatalyst was nominally photodeposited onto the photocatalysts using a K_2PtCl_4 precursor. Finally, the amount of the evolved gas was calculated after 5 h (1st h was excluded) of irradiation according to the Clausius–Clapeyron relation (PV = nRT).

Photocatalytic H_2O_2 Production

Sacrificial photocatalytic H_2O_2 production experiments were performed in a 4 mL vial reactor. First, 5 mg of catalyst was dispersed in 2 mL of a 3.5% w/w glycerin aqueous solution then O_2 gas was bubbled for 1 min. The reactor was then irradiated under stirring using two purple LED lamps (50 W each, λ = 410 nm) for 1 h. The suspension was then centrifuged at 10 000 rpm for 10 min to separate the catalysts from the solution. The generated H_2O_2 was quantified spectrophotometrically following the titanium oxalate method previously reported in the literature.[4] Basically, a 10 g L^{-1} solution of $K_2[TiO(C_2O_4)_2]\cdot 2H_2O$ was prepared using 450 mL of water and 50 mL of sulfuric acid to avoid the complex precipitation. Subsequently, 3 mL of this reagent was mixed with 1 mL of the supernatant from the photocatalytic experiment. The resulting solutions, properly diluted when needed, were analyzed using the UV–vis spectrometer, collecting absorbance values at 400 nm. A calibration curve was made with external samples of known H_2O_2 concentrations between 0-10 mmol L^{-1} with a linear analytical response (R^2 = 0.99996).

Apparent Quantum Yield (AQY) Estimation

The AQY was measured using a monochromatic visible light (410 ± 1.0 nm). The AQY was obtained by the following equation:

$$AQY\ (\%) = \frac{2 \times r_{product} \times N_A \times hc}{I \times A \times \lambda} \times 100$$

where $r_{product}$ is the production rate of H_2 or H_2O_2 molecules (mol s^{-1}) after the 1st hour of photocatalytic reaction , N_A is Avogadro constant (6.022×10^{23} mol^{-1}), h is the Planck constant (6.626×10^{-34} J s^{-1}) multiplied by c the speed of light (3×10^8 m s^{-1}) giving ($1.98644586 \times 10^{-25}$ J m), A is the irradiation area (cm^2), I is the intensity of irradiation light (W cm^{-2}), and λ is the wavelength of the monochromatic light (m).

5. (Photo)electrochemical Tests

All (photo)electrochemical measurements were carried out in a three-electrode configuration, with a Pt coil and Ag/AgCl as counter and reference electrodes, respectively.

Electrocatalytic Hydrogen Evolution Reaction (HER) and Oxygen Reduction Reaction (ORR) Measurements

The electrocatalysis experiments were conducted with a Gamry Interface 1010E potentiostat. To prepare the working electrode, F-doped tin oxide (FTO) glass (3 x 1 cm) substrates were cleaned sequentially with detergent, distilled H_2O and ethanol for 10 min each to remove organic impurities. Half of the FTO area was protected with a Scotch tape. A catalyst ink was obtained by mixing 5 mg of photocatalyst powder, 0.5 mL of H_2O and 20 µL of 5 wt.% Nafion by sonication. Then, 50 µL of catalyst slurry was pipetted onto the FTO electrode and dried at 65 ^oC and further heated at 120 ^oC for 1 h to improve adhesion. HER and ORR activities were measured in N_2- and O_2-saturated 0.2 M aqueous Na_2SO_4 solution, respectively. All potentials described were given in reference to the reversible hydrogen electrode (RHE).

Transient Photocurrent Response, Electrochemical Impedance Spectroscopy (EIS), and Mott-Schottky Analysis

The photocurrent response was measured (0.3 V vs. ref) under 100 mW cm^{-2} white LED illumination in 0.2 M aqueous Na_2SO_4 solution using a Gamry Interface 1010E potentiostat. For EIS, the same electrodes were used as described above and the measurements were done in a frequency range of 10 kHz to 1 Hz. The data were fitted to a full semicircle using ZView software. Mott–Schottky measurements were performed in a Biologic MPG-2 system at 10 kHz.

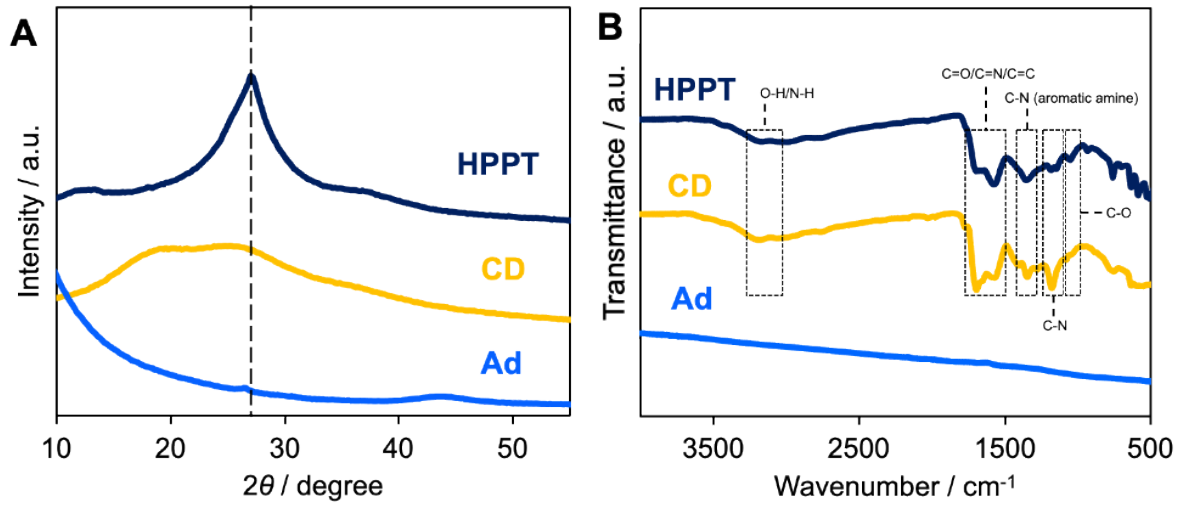

Figure S1. (A) XRD patterns and (B) FTIR spectra of Ad-carbon, CD and HPPT.

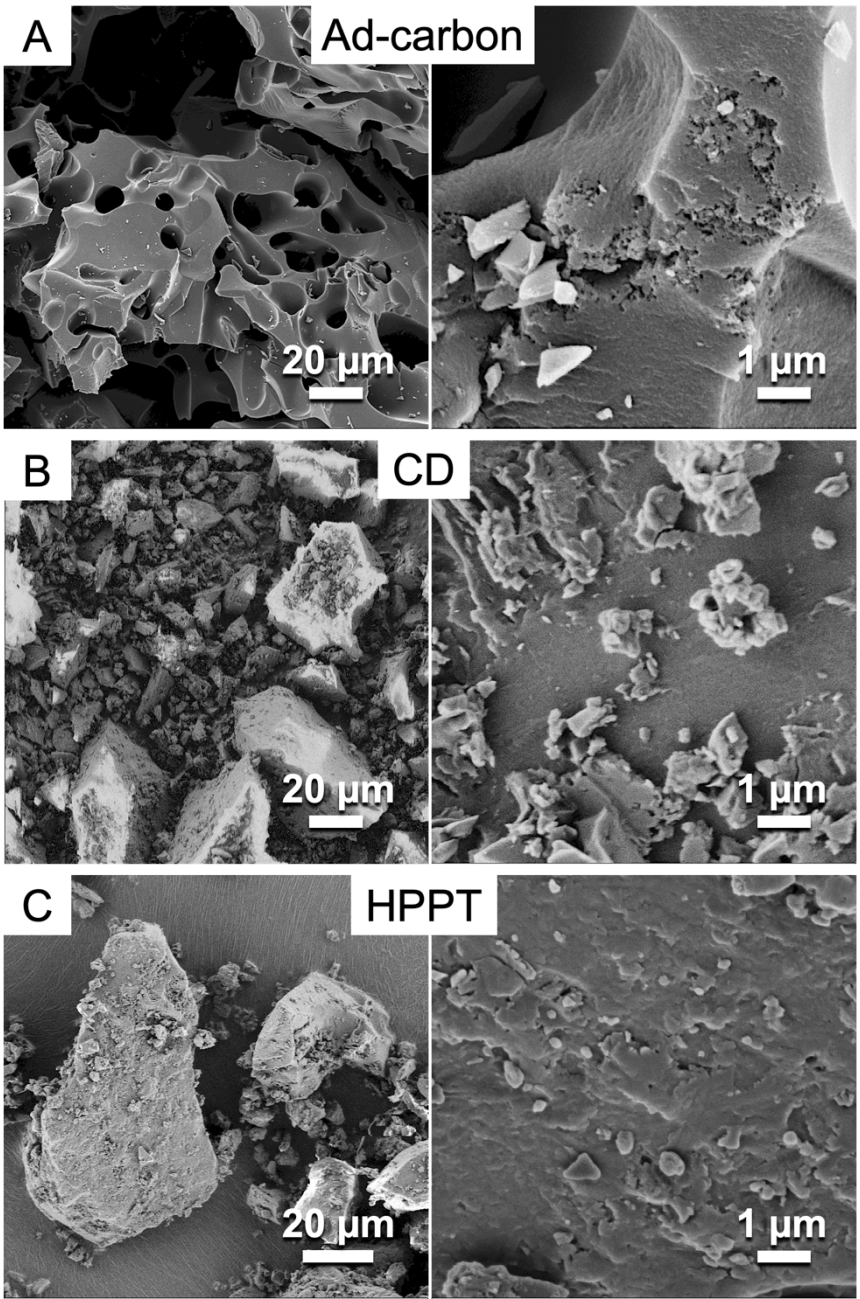

Figure S2. SEM images of various carbonaceous materials: (A) Ad-carbon, (B) CD, and (C) HPPT.

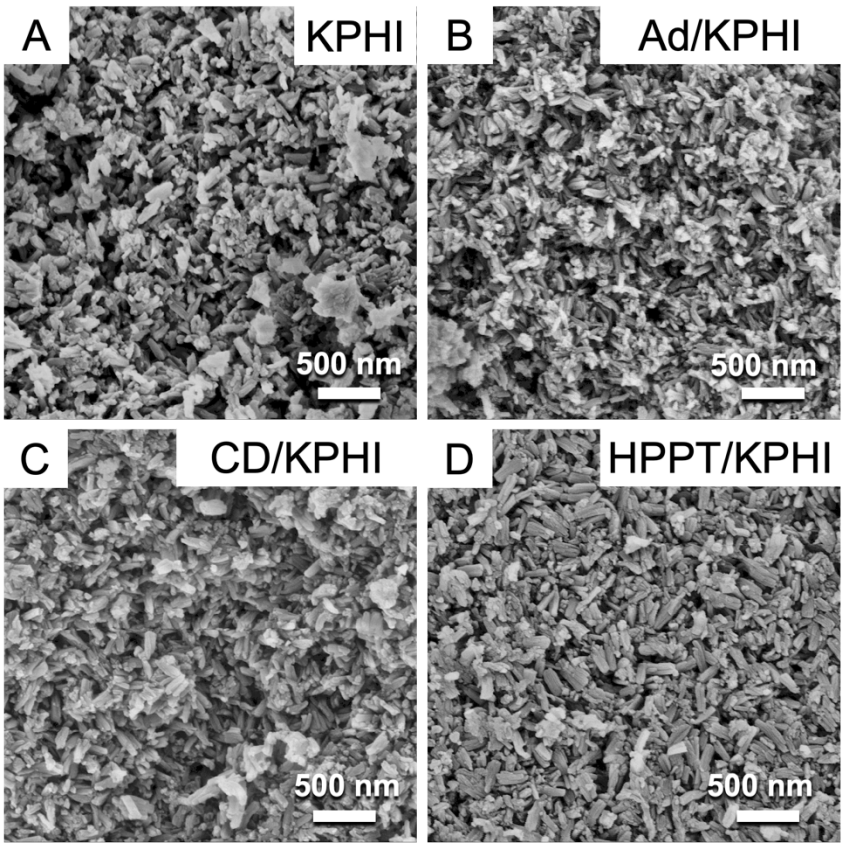

Figure S3. SEM images of (A) KPHI, (B) 0.3Ad/KPHI, (C) 0.3CD/KPHI and (D) 0.3HPPT/KPHI.

Table S1. BET specific surface area and pore diameter size of CM, KPHI and CM/KPHI hybrids

Sample	S_{BET} ($m^2\ g^{-1}$)	Pore Radius (nm)
Ad-carbon	3306	1.9
CD	1.5	1.7
HPPT	1.2	1.7
KPHI	86.4	1.9
0.3Ad/KPHI	79.7	1.9
$0.3CD_m$/KPHI	73.1	1.9
0.3HPPT/KPHI	52.9	1.9

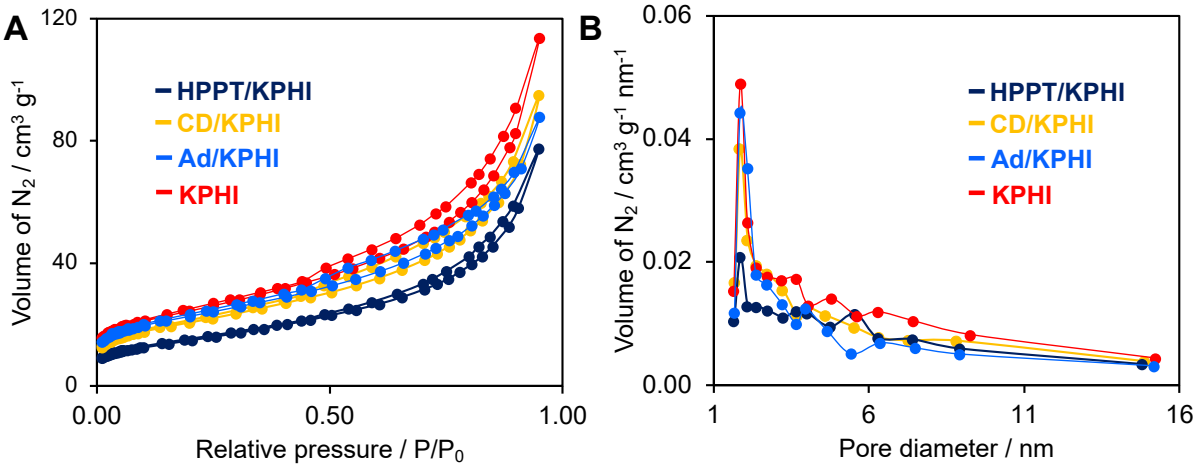

Figure S4. (A) N_2 adsorption/desorption isotherm at 77 K and (B) BJH pore size distribution from the N_2 adsorption branch at 77 K of the KPHI and CM/KPHI hybrids.

Table S2. Chemical composition of KPHI and CM/KPHI hybrids*

Sample	N %	C %	H %	C/N mass	C/H mass	K %	Li %
KPHI	44.8	27.7	2.1	0.62	13.4	9.6	0.2
0.3Ad/KPHI	45	27.7	2.2	0.62	12.8	9.6	0.2
0.3CD_m/KPHI	44.8	28	2.2	0.62	12.6	11.1	0.2
0.3HPPT/KPHI	45	27.5	2.1	0.61	12.9	9.9	0.2

*Mass percentages of N, C and H elements were measured using combustion analysis while inductively coupled plasma optical emission spectrometry (ICP-OES) was used for determining the mass percentages of K and Li.

Table S3. Comparison of H_2 evolution rates of different carbon nitride-based photocatalysts reported in the literature

Samples	Light source	Amount of catalyst /Cocatalyst	HER rate /μmol h^{-1} g_{cat}^{-1}	Reference
0.3Ad/KPHI	**50 W LED lamp (> 420 nm)**	**50 mg/3 wt% Pt**	**738**	**This work**
KPHI	300 W Xe lamp (> 420 nm)	14-20 mg/ 8 wt% Pt	600	5
$CNB_{0.2}$	500 W HBO lamp (> 420 nm)	100 mg/ 3 wt% Pt	300	6
OCNA-6	300 W Xe lamp (> 420 nm)	25 mg/3 wt% Pt	663	7
ONLH-600	300 W Xe lamp (> 420 nm)	30 mg/5 wt% Pt	340	8
P-TCN	300 W Xe lamp (> 420 nm)	100 mg/1 wt% Pt	670	9

HTCN-500	350 W Xe lamp	20 mg/3 wt% Pt	890	10
PTYS CN-2	300 W Xe lamp (> 420 nm)	50 mg/1 wt% Pt	740	11
PCNT-3	300 W Xe lamp (> 420 nm)	50 mg/3 wt% Pt	2020	12
CN-NaK	50 W LED lamp (> 420 nm)	50 mg/3 wt% Pt	5560	13

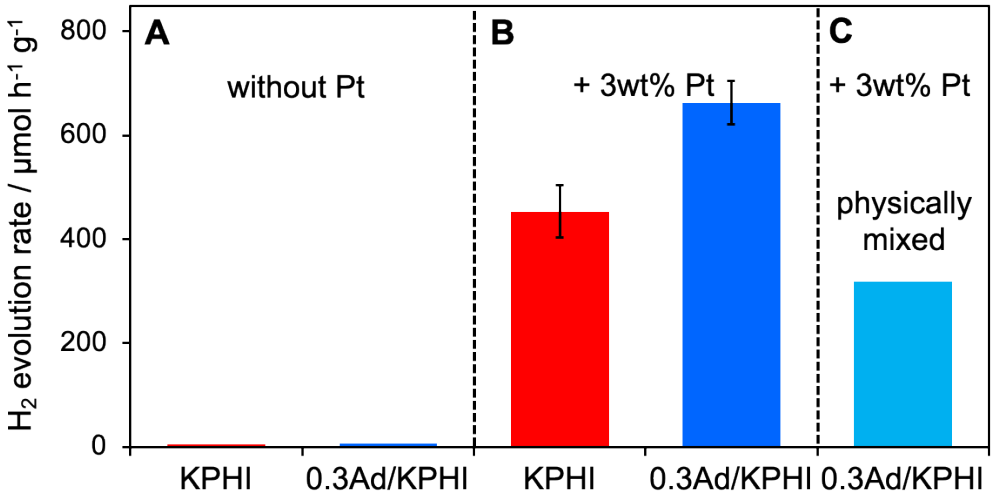

Figure S5. Photocatalytic H_2 evolution rates of pure KPHI and 0.3Ad/KPHI (A) without and (B) with 3 wt% Pt cocatalyst. (C) Photocatalytic H_2 evolution rate of a simple mixture of Ad-carbon and KPHI. Reaction conditions: catalyst, 50 mg; solution, 38 mL H_2O (10 vol% TEOA); light source, white LED (λ > 420 nm). By considering that ~150 mg of 0.3Ad/KPHI photocatalyst powder is produced from one-step salt-melt assisted condensation of 0.3 mg Ad

with 1 g 5-aminotetrazole and assuming that all of Ad-carbon remained in the sample after washing, the physically mixed sample was prepared by grinding 0.3 mg of Ad-carbon with 150 mg of pure KPHI with an agate mortar and pestle.

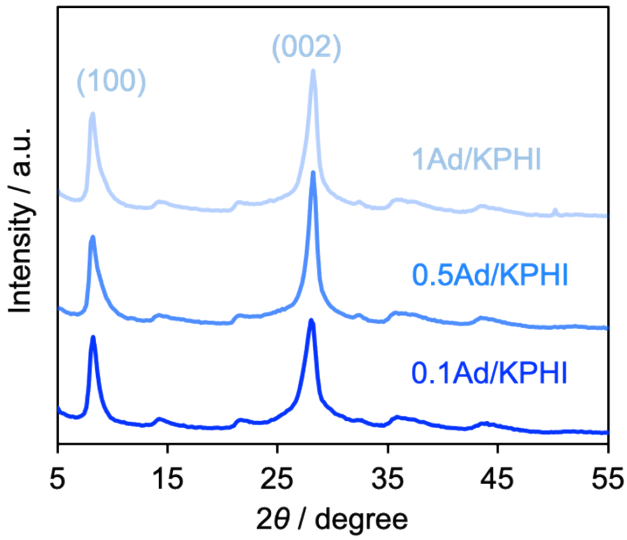

Figure S6. XRD patterns of Ad/KPHI hybrid with 0.1, 0.5 and 1 mg of Ad-carbon vs 1 g of 5-aminotetrazole.

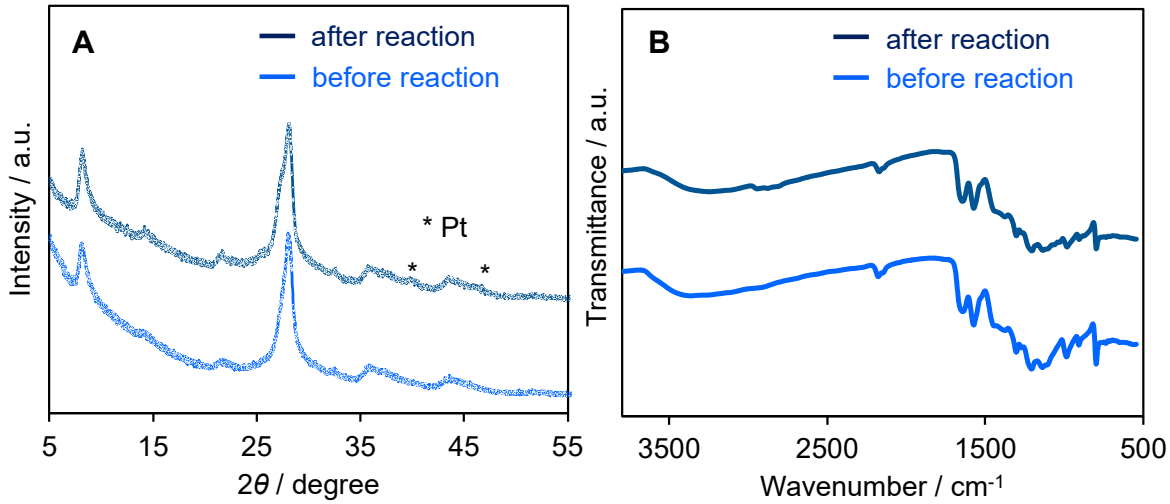

Figure S7. (A) XRD patterns and (B) FTIR spectra of 0.3Ad/KPHI before and after H_2 evolution recyclability tests.

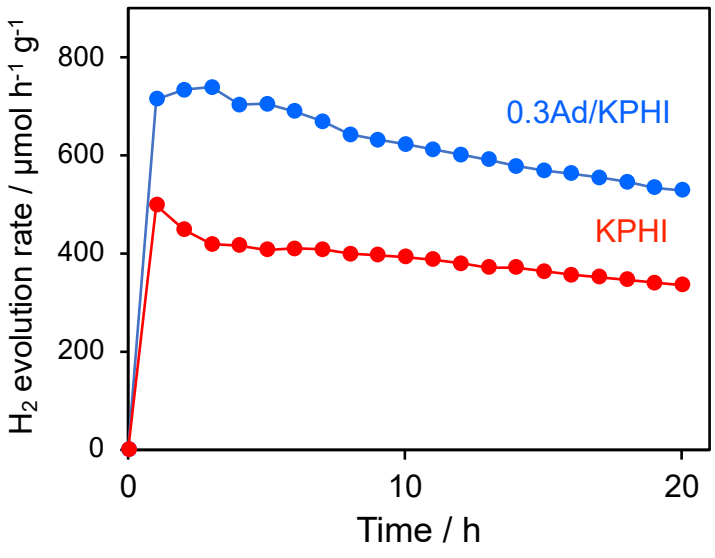

Catalysts	Light source	Sacrificial electron donor	H_2O_2 rate /mmol h^{-1} g_{cat}^{-1}	Volume (mL)	Reference
0.3Ad/KPHI	**100 W LED lamp (410 nm)**	**Glycerin**	**3.94**	**2**	**This work**
H-PHI	100 W LED lamp (410 nm)	Glycerin	3.11	2	14
KPHI	**100 W LED lamp (410 nm)**	**Glycerin**	**3.02**	2	**This work**
Na-PHI	100 W LED lamp (410 nm)	Glycerin	2.15	2	14
O/K-CN	300 W Xe lamp (> 420 nm)	2-Propanol	15.45	50	15
ACNN	300 W Xe lamp (> 420 nm)	2-Propanol	10.2	50	16
OCN/NBS	Xe lamp	2-Propanol	4.46	50	17

Figure S8.Time course of the photocatalytic H_2 evolution rates of pure KPHI and 0.3Ad/KPHI in the long-term durability test. Reaction conditions: catalyst, 50 mg; solution, 38 mL H_2O (10 vol% TEOA); cocatalyst, 3 wt% Pt; light source, white LED ($\lambda > 420$ nm).

Table S4. Comparison of H_2O_2 production rates of different carbon nitride-based photocatalysts reported in the literature

TiO_2	450 W high pressure Hg lamp (> 280 nm)	Benzyl alcohol	0.33	5	18
$Cd_3(C_3N_3S_3)_2$	300 W Xe lamp (> 420 nm)	Methanol	0.55	20	19
PCN-NaCA-2	100 mW cm^{-2} Solar simulator	Glycerin	18.7	50	20
CNK-0.8	30.7 mW cm^{-2} LED light	Ethanol	4.43	5	21
C-P-CN	300 W Xe lamp (> 400 nm)	Ethanol	3.32	50	22

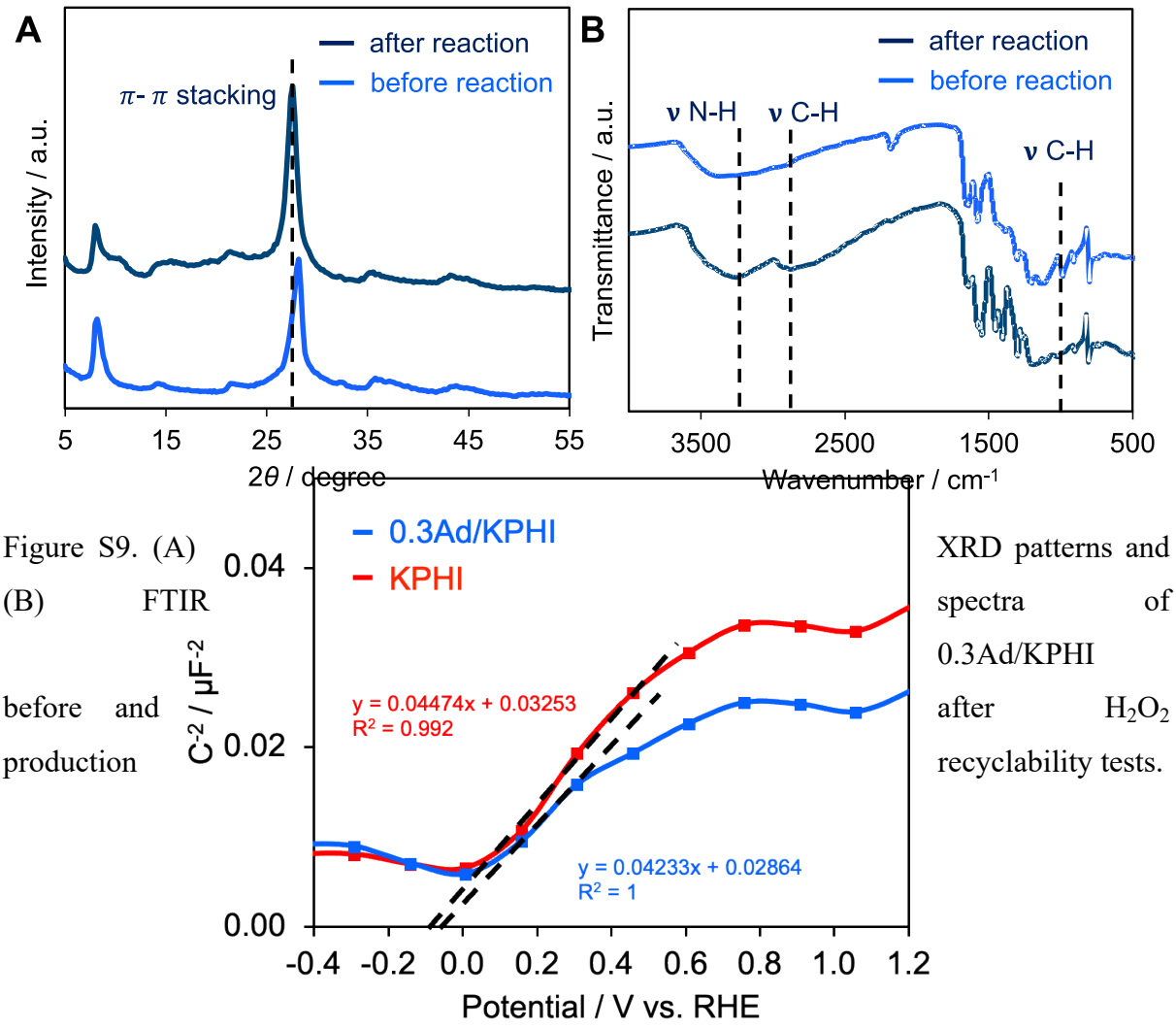

Figure S9. (A) XRD patterns and (B) FTIR spectra of 0.3Ad/KPHI before and after H_2O_2 production recyclability tests.

Figure S10. Mott-Schottky plots of KPHI and 0.3Ad/KPHI.

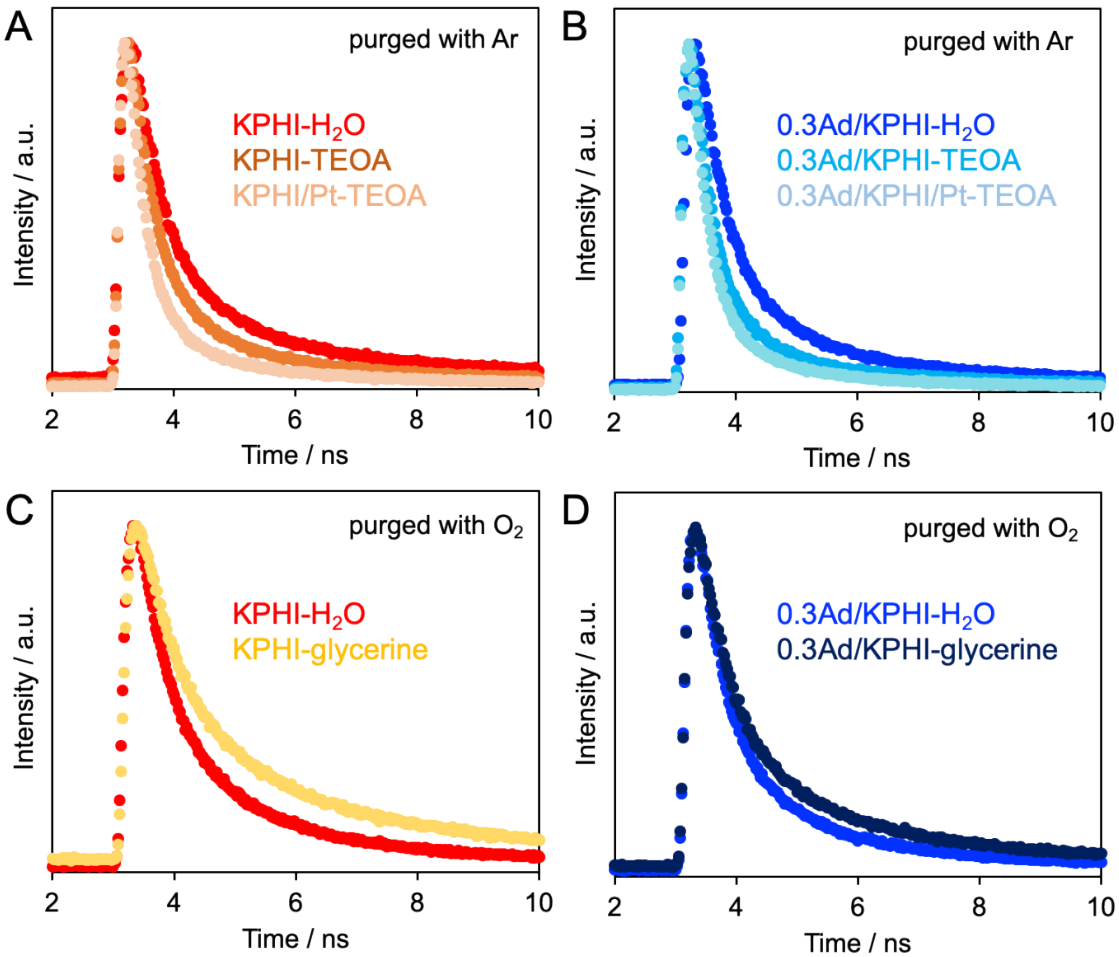

Figure S11. Time-resolved transient PL decay curves of KPHI and 0.3Ad/KPHI in aqueous suspensions under different conditions.

Sample	A_1	τ_1 (ns)	A_2	τ_2 (ns)	A_3	τ_3 (ns)	τ_{ave} (ns)	Purged Gas
KPHI-H_2O	16.98	0.15	1.54	4.11	6.92	0.83	2.14	Ar
KPHI-TEOA	26.7	0.10	1.07	4.17	6.56	0.69	1.87	
KPHI/Pt-TEOA	44.6	0.07	0.71	4.61	4.69	0.60	1.81	
0.3Ad/KPHI-H_2O	19.6	0.13	1.37	3.97	7.05	0.77	1.94	
0.3Ad/KPHI-TEOA	37.4	0.08	0.84	4.30	5.84	0.63	1.75	
0.3Ad/KPHI/Pt-TEOA	42.7	0.08	0.57	4.18	4.26	0.63	1.40	
KPHI-H_2O	15.5	0.15	1.84	3.67	7.34	0.87	1.99	O_2
KPHI-glycerine	12.34	0.14	3.11	4.28	6.96	0.94	2.93	
0.3Ad/KPHI-H_2O	18.77	0.14	1.35	4.03	6.73	0.84	1.96	
0.3Ad/KPHI-glycerine	17.18	0.12	2.22	3.94	7.1	0.80	2.37	

Table S5. PL lifetime values of KPHI and 0.3Ad/KPHI in aqueous suspension under different experimental conditions.

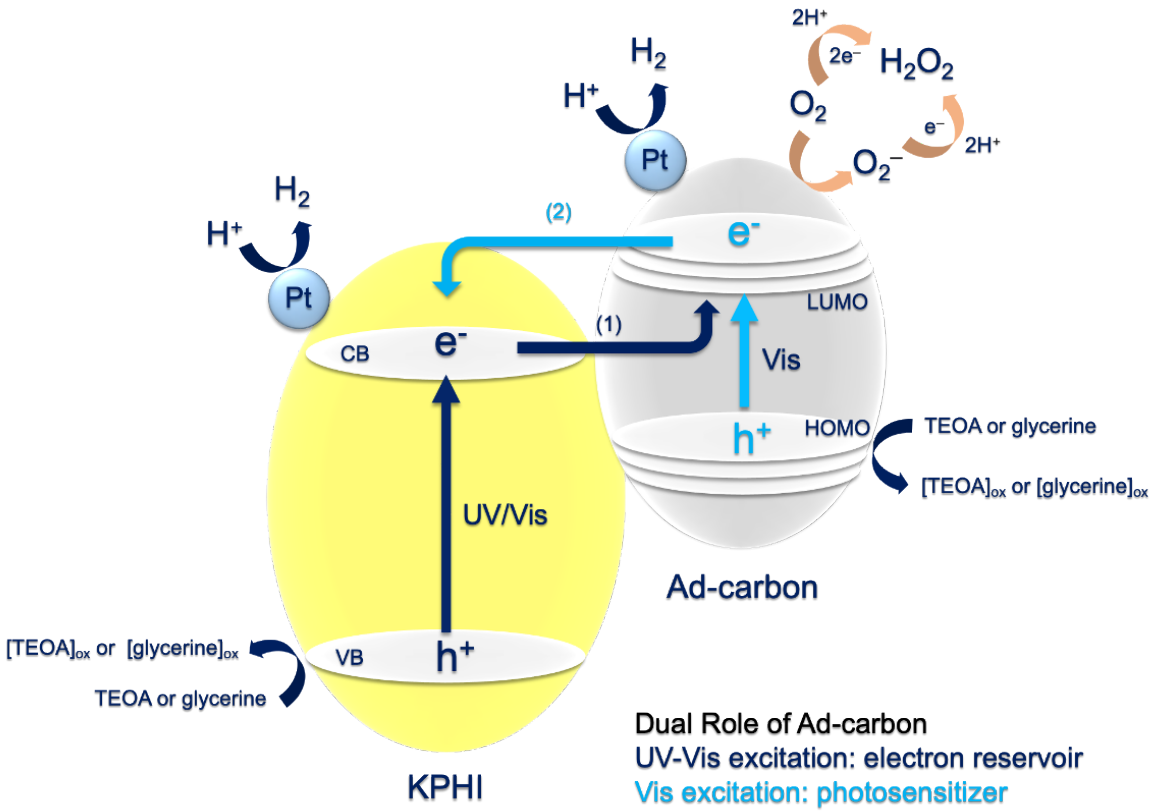

Figure S12. Schematic illustration of photocatalytic H_2 and H_2O_2 evolution over the 0.3Ad/KPHI hybrid photocatalyst system.

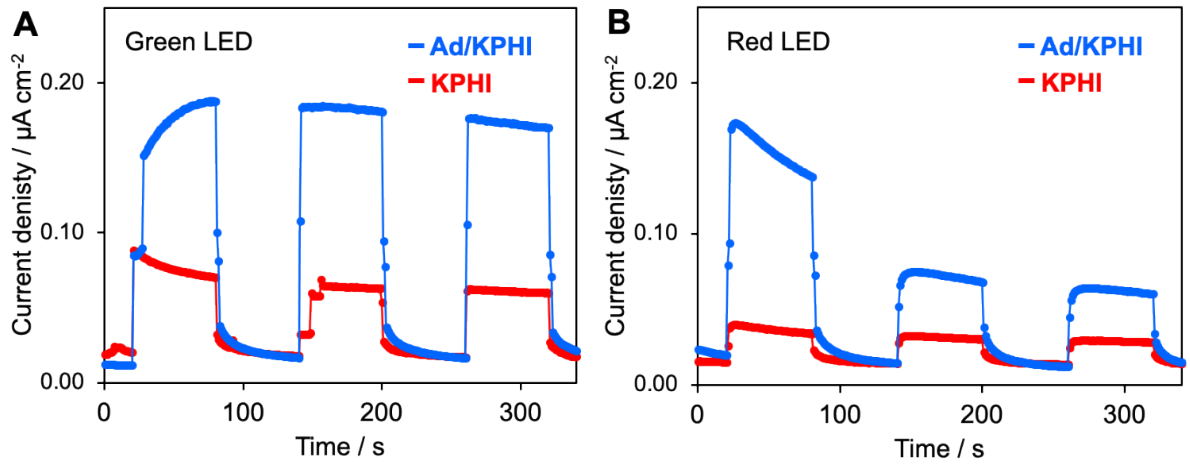

Figure S13. Transient photocurrent (applied potential 0.3 V) for KPHI and 0.3Ad/KPHI in 0.2 M Na_2SO_4 aqueous solution under (A) green and (B) red LED illumination.

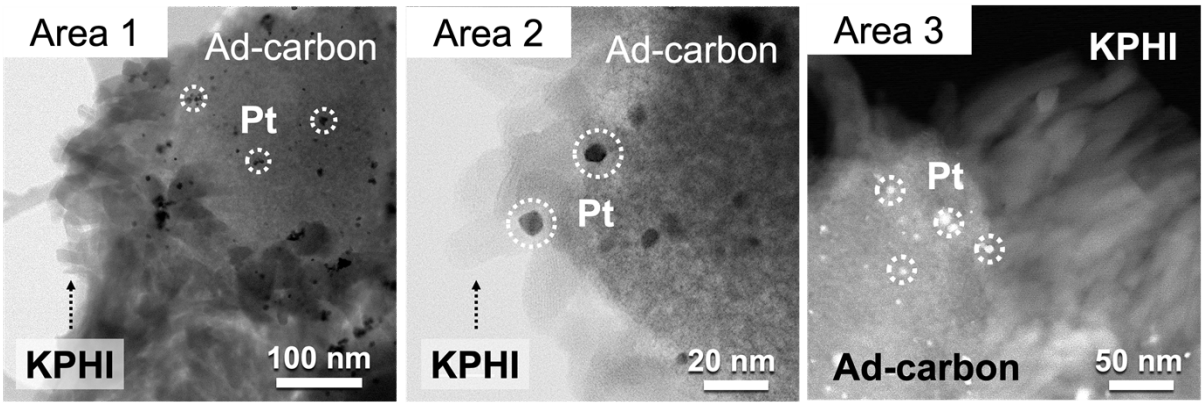

Figure S14. Additional BF- and HAADF-STEM images showing various random areas of 3Ad/KPHI hybrid sample (Ad-carbon concentration is increased by 10x to easily locate the heterostructure).

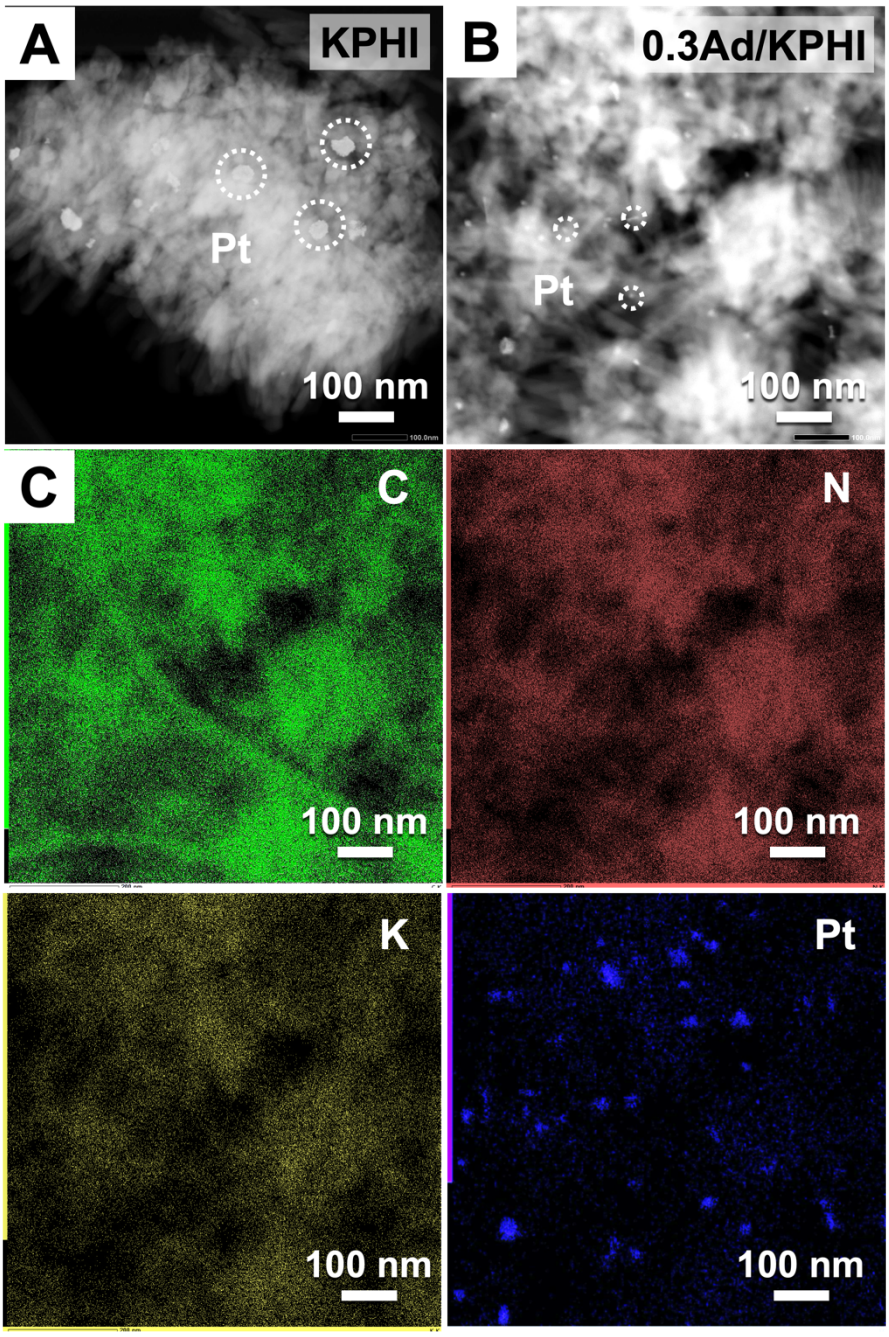

Figure S15. Additional HAADF-STEM images of (A) KPHI and (B) 0.3Ad/KPHI hybrid sample. (C) STEM-EDX elemental mapping images of (B).

References

1. J. Li, J. Kossmann, K. Zeng, K. Zhang, B. Wang, C. Weinberger, M. Antonietti, M. Odziomek and N. López-Salas, *Angew. Chem. Int. Ed.* 2023, e202217808.
2. Y. Wang, X. Liu, X. Han, R. Godin, J. Chen, W. Zhou, C. Jiang, J. F. Thompson, K. B. Mustafa, S. A. Shevlin, J. R. Durrant, Z. Guo and J. Tang, *Nat. Commun.*, 2020, **11**, 2531.
3. A. Savateev , D. Dontsova , B. Kurpil and M. Antonietti , *J. Catal.*, 2017, **350** , 203–211.
4. R. M. Sellers *Analyst*, 1980, **105**, 950–954.
5. H. Schlomberg, J. Kröger, G. Savasci, M. W. Terban, S. Bette, I. Moudrakovski, V. Duppel, F. Podjaski, R. Siegel, J. Senker, R. E. Dinnebier, C. Ochsenfeld and B. V. Lotsch, *Chem. Mater.* **2019**, 31 (18), 7478–7486.
6. J. Zhang, X. Chen , K. Takanabe, K. Maeda, K. Domen, J. D. Epping, X. Fu, M. Antonietti and X. Wang, *Angew. Chem. Int. Ed.*, **2010**, 49 (2), 441–444.
7. W. Jiang, Q. Ruan, J. Xie, X. Chen, Y. Zhu and J. Tang, *Appl. Catal. B: Environ.* **2018**, *236*, 428–435.
8. Y. Wang, M. K. Bayazit, S. J. A. Moniz, Q. Ruan and J. Tang, *Energ. Environ. Sci.* **2017**, *10*, 1643-1651.
9. S. Guo, Z. Deng, M. Li, B. Jiang, C. Tian, Q. Pan and H. Fu, *Angew. Chem. Int. Ed. Engl.* **2016**, *55*, 1830–1834.
10. Y. Li, F. Gong, Q. Zhou, X. Feng, J. Fan and Q. Xiang, *Appl. Catal. B: Environ.* **2020**, *268*, 118381
11. N. Tian, K. Xiao, Y. Zhang, X. Lu, L. Ye, P. Gao, T. Ma and H. Huang, *Appl. Catal. B: Environ.* **2019**, *253*, 196–205.
12. M. Wu, J. Zhang, B.-b. He, H.-w. Wang, R. Wang and Y.-s. Gong, *Appl. Catal. B: Environ.* **2019**, *241*, 159–166.
13. G. Zhang, L. Lin, G. Li, Y. Zhang, A. Savateev, S. Zafeiratos, X. Wang and M. Antonietti, *Angew. Chem. Int. Ed. Engl.* **2018**, *57*, 9372–9376.
14. A. Rogolino, I. Silva, N. Tarakina, M. da Silva, G. Rocha, M. Antonietti and I. Teixeira, *ACS Appl. Mater. Interfaces,* 2022, **14**, 44, 49820–49829.
15. W. Liu, P. Wang, J. Chen, X. Gao, H. Che, B. Liu, Y. Ao, *Adv. Funct. Mater.* 2022, **32**, 2205119.
16. S. Wu , H. Yu , S. Chen and X. Quan , *ACS Catal.*, 2020, **10** , 14380–14389.
17. F. Farzin, M. K. Rofouei, M. Mousavi, Ja. B. Ghasemi, *J. Phys. Chem. Solids* 2022, **163**, 110588.
18. Y. Shiraishi, S. Kanazawa, D. Tsukamoto, A. Shiro, Y. Sugano and T. Hirai, *ACS Catal.*, 2013, **3**, 2222–2227.
19. H. Zhuang, L. Yang, J. Xu, F. Li, Z. Zhang, H. Lin, J. Long, X. Wang, *Sci. Rep.* 2015, **5**, 16947.
20. Y. Zhao , P. Zhang , Z. Yang , L. Li , J. Gao , S. Chen , T. Xie , C. Diao , S. Xi , B. Xiao , C. Hu and W. Choi , *Nat. Commun.*, 2021, **12** , 3701.
21. Z. Li, Y. Chen, X. Chen, L. Li, S. Kuang, Y. Guo, Y. Wang, J. Gao, *Appl. Surf. Sci.* 2023, **609**, 155432.
22. W. Wei, L. Zou, J. Li, F. Hou, Z.Sheng, Y. Li, Z. Guo, and A. Wei, *J. Colloid Interface Sci.*, 2023, **636**, 537–548.